

Clausius' Virial vs. Total Potential Energy in the dynamics of a two-component system.

C. Marmo and L. Secco

Department of Astronomy, University of Padova, Padova, Italy

Abstract

In a gravitational virialized bound system built up of two components, one of which is embedded in the other, the Clausius' virial energy of one subcomponent is not, in general, equal to its total potential energy, as occurs in a single system without external forces. This is the main reason for the presence, in the case of two non-coinciding concentric spheroidal subsystems, of a minimum (in absolute value) in the Clausius' virial of the inner component B , when it assumes a special configuration characterized by a value of its semi-major axis we have named *tidal radius*. The physical meaning, connected with its appearance, is to introduce a scale length on the gravity field of the inner subsystem, which is induced from the outer one. Its relevance in the galaxy dynamics has been stressed by demonstrating that some of the main features of Fundamental Plane may follow as consequence of its existence. More physical insight into the dynamics of a two component system may be got by looking at the location of this scale length inside the plots of the potential energies of each subsystem and of the whole system and by also taking into account the trend of the anti-symmetric residual-energy, that is the difference between the tidal and the interaction-energy of each component. Some thermodynamical arguments related to the inner component are also added to prove as special is the *tidal radius configuration*. Moreover the role of the divergency at the center of the two subsystems in obtaining this scale length is considered. For the sake of simplicity the analysis has been performed in the case of a frozen external component even if this constraint does not appear to be too relevant in order to preserve the main results.

Key words: Celestial Mechanics, Stellar Dynamics; Galaxies: Clusters.

Email addresses: marmo@pd.astro.it, secco@pd.astro.it (C. Marmo).

1 Introduction

In order to understand the dynamics of a two-component system which a galaxy is, during its virial evolution, we need to explain what the trends of the Clausius' Virial and of the total potential energy of each subsystem, together with that of the whole system, are, as soon as the inner (baryonic) component contracts inside the potential well of the outer dark matter halo. In spite of the limits of this model which, of course, is able to reproduce only some essential features of a real galaxy, its relative analytical simplicity, due to the use of tensor virial theorem, provides us with a powerful tool for understanding the role of the physical parameters involved in the dynamic evolution of a real system. For the sake of simplicity we will assume that the outer component is at fixed size and shape without considering this constraint to be too essential in order to determine the main features of the dynamic evolution we are dealing with (see, (Secco, 2001) , hereafter LS1). Indeed the masses of the two components are not equal, the outer one being about ten times the inner one. As a consequence, tidal influences between the subsystems are not symmetric; that acting from inner to the outer is actually weaker than the reverse (Caimmi & Secco 1993). Even if a contraction effect is induced from inner density distribution on the inner regions of outer halo, during the dynamical evolution, as already underlined by Barnes & White (1984) , that effect seems, indeed, does not cause a dramatic modification of the outer mass distribution, if there is a supernovae- driven outflow, according to some recent N-body simulations (Lia et al. 2000). On the other side, models in which this constraint has been changed with some less stringent additional conditions (Caimmi 1994), seem to prove the same conclusion. Then, in order to underline the main effect of inducing a tidal scale length from the dark halo over the luminous component, we will neglect this possible modification. It seems to us that this may correspond to change from a given mass distribution to an other with a new exponent d (see, sect.3) not too different from the previous one; that might be included in the different cases considered without cancelling the effect we are dealing with.

The two subsystems will be modelled by two penetrating similar-strata spheroids with two power-law density profiles. The advantage of this model is to be able to handle all the energetics of a two-component system during its dynamic evolution in an analytical way. Nevertheless to obtain some physical meaningful relationships, we prefer to sacrifice the more correct, but very boring, exact analytical expressions and to use some suitable mathematical approximations. Through them it will be possible to describe the whole virial evolution by means of relatively simple equations which involve only the two exponents (b and d of sect.3) which characterize the two subsystem power-law density distributions (B , the inner and D the outer, respectively), as soon as the common form factor F of sect.3 is fixed ($=2$, in the spherical case). The appearance

of a non-monotonic trend for the inner Clausius' virial energy, the contrary of that which refers to the inner total potential energy, is the most important result for the dynamics of a two-component system during its virial phase. Its relevance has already been stressed by demonstrating how some of the main features of elliptical galaxy Fundamental Plane may follow as a consequence of it (LS1). Its occurrence seems to be a general feature when one component is completely embedded in another. This has also been tested by considering different models from those taken into account here as such the case of heterogeneous density profiles with different eccentricities (Caimmi & Secco, 2001).

Moreover, how much the extensions of the cores, at the center of the two sub-structures, have to be in order to obtain a maximum of the virial energy in the inner component, will be investigated when the luminous matter distribution becomes particularly steep. The present scheme may be extended to other two-component systems built up of baryonic + dark matter as, e.g., the galaxy clusters are.

2 Virial and total potential energy

By referring to Caimmi & Secco (1992) and the references therein, the Clausius' virial, or virial potential energy, V_u ($u = B, D$), appears with the kinetic energy, T_u , in the scalar virial equations related to the two components, the inner, B , embedded in the outer, D , of a virialized system:

$$2T_u + V_u = 0. \quad (1)$$

It refers to the energy contribution due to the two active forces on the respective subsystem: the self-gravity and the tidal-gravity due to the other component.

Generally speaking, it turns out to be:

$$V_u = \Omega_u + V_{uv}, \quad (2)$$

where,

$$\Omega_u = \int \rho_u \sum_{r=1}^3 x_r \frac{\partial \Phi_u}{\partial x_r} d\vec{x}_u, \quad (3)$$

and

$$(V_{uv}) = \int \rho_u \sum_{r=1}^3 x_r \frac{\partial \Phi_v}{\partial x_r} d\vec{x}_u, \quad (4)$$

Φ_u and Φ_v being the gravitational potentials due to u -matter and v -matter distributions, respectively.

In order to obtain the total potential energy of the u -component, we have to add at the self-potential energy the interaction energy W_{uv} , i.e.:

$$(E_{pot})_u = \Omega_u + W_{uv}, \quad (5)$$

The difference between the total and the virial u -energy is:

$$V_u - (E_{pot})_u = Q_{uv}, \quad (6)$$

Q_{uv} being the residual energy, which is anti-symmetric with respect to the exchange of one component with the other. The following equations also hold:

$$V_{uv} = W_{uv} + Q_{uv}, \quad (7)$$

$$W_{uv} = W_{vu}; \quad (8)$$

the latter shows the symmetry of the interaction energy tensor.

As consequence, the total potential energy tensor trace of the whole system, in the principal inertia axes frame of reference, is expressed by:

$$E_{pt} = (E_{pot})_u + (E_{pot})_v = \Omega_u + \Omega_v + W_{uv} + W_{vu} = V_u + V_v. \quad (9)$$

It should be underlined that the residual energy may become zero, and then the total potential energy of each subsystem is equal to the Clausius' virial energy, only for some specific configurations which depend on the mass distributions of the two subsystems (see, sect.7).

3 Similar and similar-strata spheroids

According to Caimmi (1993) (hereafter RC) and to Secco (2000) (hereafter LS), we consider, now, the case of two similar spheroids (that means, with the same axis ratio $\epsilon_B = \epsilon_D = \epsilon$ (then the same form factor $F = (2\frac{\alpha(\epsilon)}{\epsilon} + \frac{\epsilon^2\gamma(\epsilon)}{\epsilon})$),

with similar and coaxial strata mass distributions. We set the radial density profiles according to two power-laws as follows:

$$\rho_B \sim \frac{1}{r^b}, \quad (10)$$

$$\rho_D \sim \frac{1}{r^d}; \quad (11)$$

and to avoid the central divergence we add an inner homogeneous core to both mass distributions. For the sake of simplicity we assume here that these two cores have the same extension (ξ_c) in the a -dimensional coordinates (see, RC). Then, the traces of B and D self-potential energy tensors are, respectively:

$$\Omega_B = -\nu_{\Omega B} \frac{GM_B^2}{a_B} F, \quad (12)$$

$$\Omega_D = -\nu_{\Omega D} \frac{GM_D^2}{a_D} F. \quad (13)$$

where M_u is the mass and a_u the semi-major axis of the considered subsystem. The coefficient $\nu_{\Omega u}$ depends on the mass distribution via the functions h and g_{3u} , from Table 1 of the Appendix A in RC.

The traces of B and D tidal-potential energy tensors are:

$$V_{BD} = -\nu_V \frac{GM_B^2}{a_B} F, \quad (14)$$

$$V_{DB} = -\nu_{VD} \frac{GM_D^2}{a_D} F. \quad (15)$$

The symmetric interaction energy tensor trace is

$$W_{BD} = -\nu_W \frac{GM_B^2}{a_B} F. \quad (16)$$

The following expressions define the ν -coefficients of the previous energies:

$$\nu_V = -\frac{9}{8} [(\nu_B)_M (\nu_D)_M]^{-1} m w^{ext}(x), \quad (17)$$

$$\nu_{VD} = -\frac{9}{8} [(\nu_B)_M (\nu_D)_M]^{-1} \frac{1}{mx} w^{int}(x), \quad (18)$$

$$\nu_W = -\frac{9}{16} [(\nu_B)_M (\nu_D)_M]^{-1} m [w^{int}(x) + w^{ext}(x)], \quad (19)$$

where $x = a_B/a_D$ e $m = M_D/M_B$. The $(\nu_u)_M$ coefficients are defined in Tab. 1 of RC. Due to the eqs.(17, 19) the following relation also holds:

$$W_{BD} = \frac{9}{16}[(\nu_B)_M(\nu_D)_M]^{-1}m w^{int}(x)\frac{GM_B^2}{a_B}F + \frac{1}{2}V_{BD} \quad (20)$$

The definitions of $w^{int}(x)$ and $w^{ext}(x)$ and their approximations are given in the Appendix.

It should be stressed that w^{ext} contains the expression of the D -mass fraction which has dynamical effect over the B -component at every value of x (see Appendix).

4 Dynamical quantities

In order to gain some physical meaningful relationships, we will adopt here some mathematical simplifications. It should be underlined that all the approximations we consider in the following section and in the Appendix, refer to the case in which the two cores have the same a-dimensional extension ξ_c and under the limitation that $x > \xi_c$. In a further paper we will relax these constraints.

Under the approximations we have considered in the Appendix, eq.(14) becomes:

$$V_{BD} \simeq -\nu'_V G \frac{M_B \widetilde{M}_D}{a_B} F \quad (21)$$

B -Clausius' virial may be defined as:

$$V_B \simeq GM_B^2 F \left[-\nu_{\Omega B} \frac{1}{a_B} - \nu'_V \frac{M_D}{M_B} \frac{1}{a_D} \left(\frac{a_B}{a_D} \right)^{2-d} \right] \quad (22)$$

or in normalized form:

$$\widetilde{V}_B = \frac{V_B a_D}{GM_B^2 F} \simeq -\frac{\nu_{\Omega B}}{x} - \nu'_V \left(\frac{M_D}{M_B} \right) x^{2-d}; \quad x = \frac{a_B}{a_D} \quad (23)$$

By using the eq.(20) and the approximation (A.14) ($\epsilon \simeq 0$) we obtain:

$$W_{BD} \simeq -\frac{9}{4}[(\nu_B)_M(\nu_D)_M]^{-1} \frac{GM_B M_D}{a_D} \frac{\xi_c^{b+d}}{(2-d)(3-b)} F - \frac{1}{2(2-d)} V_{BD} \quad (24)$$

and from eq.(7):

$$Q_{BD} \simeq \frac{9}{4}[(\nu_B)_M(\nu_D)_M]^{-1} \frac{GM_B M_D}{a_D} \frac{\xi_c^{b+d}}{(2-d)(3-b)} F + \frac{5-2d}{2(2-d)} V_{BD} \quad (25)$$

Finally from the definition of $(E_{pot})_B$ (eq.(5)) and by the approximations of eqs.(24, 21), we have:

$$\begin{aligned} (E_{pot})_B &\simeq \Omega_B - \frac{9}{4}[(\nu_B)_M(\nu_D)_M]^{-1} \frac{GM_B M_D}{a_D} \frac{\xi_c^{b+d}}{(2-d)(3-b)} F \\ &\quad + \frac{\nu'_V}{2(2-d)} G \frac{M_B^2 m}{a_B} \left(\frac{a_B}{a_D}\right)^{3-d} F \end{aligned} \quad (26)$$

By normalization to the same factor of \widetilde{V}_B (eq.(23)), it follows:

$$(\widetilde{E}_{pot})_B \simeq -\frac{\nu_{\Omega_B}}{x} - \frac{9}{4}[(\nu_B)_M(\nu_D)_M]^{-1} m \frac{\xi_c^{b+d}}{(2-d)(3-b)} + \frac{\nu'_V}{2(2-d)} m x^{2-d} \quad (27)$$

or:

$$(\widetilde{E}_{pot})_B \simeq -\frac{\nu_{\Omega_B}}{x} - \frac{1}{2} \nu'_V m \frac{(3-d)[5-(b+d)]}{(2-d)(3-b)} + \frac{\nu'_V}{2(2-d)} m x^{2-d} \quad (28)$$

where is:

$$\widetilde{W}_{BD} = \widetilde{W}_{DB} \simeq -\frac{1}{2} \nu'_V m \frac{(3-d)[5-(b+d)]}{(2-d)(3-b)} + \frac{\nu'_V}{2(2-d)} m x^{2-d} \quad (29)$$

Moreover the residual energy of eq.(25) becomes:

$$\widetilde{Q}_{BD} = -\widetilde{Q}_{DB} \simeq \frac{1}{2} \nu'_V m \frac{(3-d)[5-(b+d)]}{(2-d)(3-b)} - \frac{(5-2d)}{2(2-d)} \nu'_V m x^{2-d} \quad (30)$$

The Clausius' virial related to the D subsystem, eq.(2), is:

$$V_D = \Omega_D + V_{DB}$$

where Ω_D and V_{DB} correspond to the eqs.(13, 15), respectively. In the limitations under which the approximation (A.15) holds, the approximative tensor trace of Clausius' virial, related to D component, becomes:

$$V_D \simeq -\nu_{\Omega_D} G \frac{M_D^2}{a_D} F - \nu'_V G \frac{M_D M_B}{a_D} F \left\{ \frac{(3-d)[5-(b+d)]}{(2-d)(3-b)} - \frac{3-d}{2-d} \left(\frac{a_B}{a_D}\right)^{2-d} \right\} \quad (31)$$

By normalization at the usual factor $\frac{GM_B^2 F}{a_D}$, we obtain:

$$\widetilde{V}_D \simeq -\nu_{\Omega D} m^2 - \nu'_V m \frac{3-d}{2-d} \left\{ \frac{[5-(b+d)]}{(3-b)} - x^{2-d} \right\} \quad (32)$$

By using the definition of the total potential energy of D -component of eq.(5) and passing through the eq.(29), we obtain:

$$(\widetilde{E}_{pot})_D \simeq -\nu_{\Omega D} m^2 - \frac{1}{2} \nu'_V m \frac{(3-d)[5-(b+d)]}{(2-d)(3-b)} + \frac{\nu'_V}{2(2-d)} m x^{2-d} \quad (33)$$

The definition of total potential energy of the whole system, eq.(9), yields the following normalized and approximate expression:

$$\widetilde{E}_{pt} \simeq -\frac{\nu_{\Omega B}}{x} - \nu_{\Omega D} m^2 - \nu'_V m \frac{(3-d)[5-(b+d)]}{(2-d)(3-b)} + \frac{\nu'_V}{(2-d)} m x^{2-d} \quad (34)$$

As a concluding remark of this section we wish open the question of which is the weight of the approximations on the trends of the energies if they are compared with those coming from the rigorous analytical expressions. This is remarkable (see the next section) when it refers to the non-monotonic character of the luminous Clausius' virial energy which turns out to be of extreme importance for the dynamics of the two-component system. Generally speaking, the approximations considered ($b < 2$) are as good as $\xi_c \rightarrow 0$ (e.g., the maximum score for the main physical quantities of Tab.1 is of 0.5% if $\xi_c = 0.01$ and $b = 1.5$), and that will constraint us to explore what happens on this limit.

5 Luminous component energy trends

We will analyze the trends of the two energies, the Clausius' virial of eq.(2) and the total potential energy of eq.(5) normalized by the factor $\frac{FGM_B^2}{a_D}$, which correspond to the B component mass distribution (here assumed to be the luminous one). They are approximated by the eq.(23) and the eq.(28) respectively. The related rigorous functions are:

$$\widetilde{V}_B = -\frac{\nu_{\Omega B}}{x} - \frac{\nu_V}{x} \quad (35)$$

and:

$$(\widetilde{E}_{pot})_B = -\frac{\nu_{\Omega B}}{x} - \frac{\nu_W}{x} \quad (36)$$

Their corresponding trends are given in the Fig.1 for the cases 2) and 4) of Table 1, by assuming $\xi_c = 0.01$ and $m = 8.5$. From the comparison between the values of the main physical quantities of Tab.1, which are evaluated by using the rigorous trends shown in the figures, and those yielded by the approximate formulae, the conclusion is that the errors are less than 0.5%. This maximum error is reached only in the case 4).

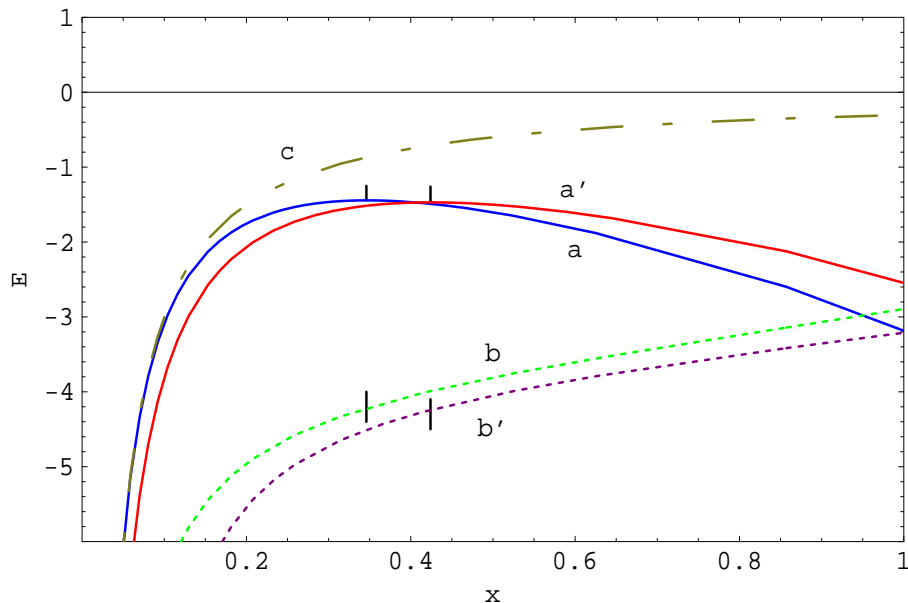


Fig. 1. The energy trends of the B -system as function of $x = a_B/a_D$, normalized at the factor $(GM_B^2 F)/a_D$. The a -curve (solid line) represents the Clausius' virial energy, \tilde{V}_B , and the b -one (dotted line), the total potential energy, \tilde{E}_B , (case 2) of Tab.1); a' and b' are the corresponding curves for the case 4) of Tab.1. For comparison the c -curve (long short-dashed line) is the self-energy trend of a single B -component in the case 2). The vertical marks correspond to the *tidal radius* configurations.

It appears the relevant non-monotonic character of the Clausius' virial energy (curves a , a') in respect to the monotonic one of the total potential energy of the same component (curves b , b').

As already shown (see, LS and LS1), when we describe a gravitational structure as in section 3, a configuration which minimizes the Clausius' virial of inner component exists, if the outer density distribution is described by a power law with an exponent less than 2. This special configuration of the embedded component is also analytically defined by the d'Alembert's Principle of virtual works. The condition of virial equilibrium means that, if the virial energy has a minimum (in absolute value), the total kinetic energy also exhibits a minimum. This implies, in turn, that if the kinetic energy of the inner bright component is dominated by the random velocity dispersion (as in ellipticals) the corresponding macroscopic pressure support has a minimum;

if, on the contrary, it is the rotational kinetic energy which dominates (as in the spirals), the rotation velocity distribution has to be that which is able to minimize the corresponding total ordered kinetic energy. The semi-major axis a_t , which characterizes this configuration, is a scale length acquired by the gravitational field of the inner component, typically without any. It is expressed, by deriving the approximated eq.(23) in respect to x :

$$a_t = \left(\frac{\nu_{\Omega B}}{\nu'_V} \frac{1}{(2-d)} \frac{M_B}{M_D} \right)^{\frac{1}{3-d}} a_D, \quad (37)$$

The result is the same as Hoerner (1958) found for the tidal radius of a spherical star cluster embedded in the galaxy tidal potential and represents a generalization of it. This is the reason the dimension given by the eq.(37) is named as *tidal radius*. By assuming $a_D = const.$, $M_D/M_B \simeq 10$ (on the basis of cosmological arguments) and by starting with the dynamical evolution at $a_B = a_{Bo} = a_D$ ($x=1$), we can see from eq.(23) that the ratio between the tidal-energy term (\tilde{V}_{BD} , the second one) and the self-energy term ($\tilde{\Omega}_B$, the first one) is:

$$\zeta_1 = \left(\frac{\tilde{V}_{BD}}{\tilde{\Omega}_B} \right)_{x=1} \simeq \frac{\nu'_V}{\nu_{\Omega B}} m \quad (38)$$

For all the realistic values of the couple (b,d) we have considered (see, Tab.1 and Fig.1 in LS) the ratio ζ_1 is greater than one and then the tidal-energy term is dominant with respect to the self-energy one. As a_B decreases at $a_D = const.$, the tidal-energy decreases, in absolute value, because of the decrease in D -mass inside the B -boundary, which is $M_D x^{3-d}$. Then the integral of force times the the position, V_{BD} , (21) decreases as x^{2-d} , meanwhile the self-energy increases in absolute value as x^{-1} . The balance between the self- and tidal-energy is reached at about a_t and then, when x becomes less than x_t ($= a_t/a_D$), the self-energy overwhelms the tidal-energy. The ζ_t ratio between the two energies at this minimum becomes:

$$\zeta_t \simeq \frac{1}{2-d} \quad (39)$$

The approximated eq.(23) allows us to connect analytically the x_e value at which the two energies, self and tidal, are equal with x_t . Indeed, it turns to be:

$$x_e \simeq x_t (2-d)^{\frac{1}{3-d}} \quad (40)$$

If $d = 1$ the equipartition between the two energies properly occurs at x_t .

Nevertheless the equation (37) is not the most general expression: the two components considered here are, indeed, always homothetic as a_B changes. In the homogeneous ($b = d = 0$), non similar case, when the axis ratio depends weakly on a_B , one approximative analytical expression of a_t exists (see, eq.(53) in LS). In order to look for a more general extension, as in the case of two different eccentricities with two heterogeneous density profiles, only a first order approach has been taken into account (Caimmi & Secco, 2001), because in this case the tensor, $(V_{uv})_{ij}$ ($u, v = B, D$; $i, j = x, y, z$), in an analytical form, is not yet available.

It is interesting to consider where the tidal radius is located on the energies curves, in order to gain more insight into its physical meaning. x_t (the vertical mark on curves of Fig.1,) corresponds to the beginning of the self-energy domain in the Clausius' energy trend. Indeed, as soon as $x < x_t$ both the virial and the total potential energy of the luminous component begin to increase (in absolute value) very steeply as the size decreases, with approximately the same trend of a single B -component self-energy (curve c in Fig.1). At dimension greater than x_t , the total potential energy curve of B -subsystem exhibits slopes smaller than the previous ones at $x < x_t$ (see curve b of Fig.2), by changing its concavity a little bit before $x = 1$ (the zero of the c-curve($= \frac{d^2(\tilde{E}_{pot})_B}{dx^2}$) in Fig.2). If one looks at the derivative $\frac{d(\tilde{E}_{pot})_B}{dx}$, curve b of Fig.2, it is manifest that a_t gives the scale length at which the slope of the B total potential energy changes. Indeed, if for $x < x_t$ the slope is about the same of that of a single contracting component (curve b'), as soon as $x > x_t$ the slope changes step by step in order to stabilize itself on one, which characterizes the tidal-energy domain, at about $x \simeq 3x_t \simeq 1$. It should be noted that the flex point is included inside the interval $x_t - 3x_t$ (see Tab.1, even if in the case 4), strictly speaking, the mathematical flex point does not correspond to a physical configuration in our model because its coordinate is a little bit greater than 1). For $x > x_t$ the rate at which the slope of the B total potential energy (curve c) varies is smaller than that at which the slope of same component without the potential well of dark matter (curve c') varies.

In order to understand under which conditions the flex point does appear and where it is located, we will take into account the approximation given by eq.(28). Indeed, it allows us to handle the following analytical expressions. At fixed outer component, the first and second derivative of $(\tilde{E}_{pot})_B$ are, respectively:

$$\frac{d(\tilde{E}_{pot})_B}{dx} \simeq \frac{\nu_{\Omega_B}}{x^2} + \frac{1}{2}\nu'_V m x^{1-d} \quad (41)$$

$$\frac{d^2(\tilde{E}_{pot})_B}{dx^2} \simeq -2\frac{\nu_{\Omega_B}}{x^3} + \frac{1}{2}\nu'_V m \frac{1}{x^d}(1-d) \quad (42)$$

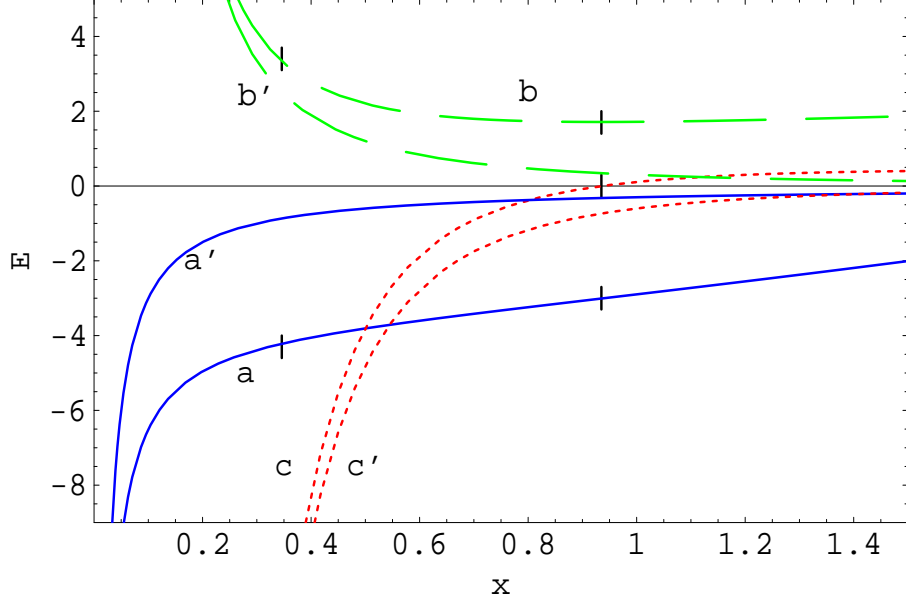


Fig. 2. Detailed potential energy trend for the B -system with and without the dark potential well, as function of x . The normalization factor is the same as in Fig.1. The a -curve (solid line) represents the total potential energy, $(\tilde{E}_{pot})_B$ in the case 2) of Tab.1; the b (long dashed line) and c (dotted line) represent the first and the second derivative of the total potential energy, respectively. b' and c' are the same derivatives for the potential energy of the single B component. The vertical marks on the left correspond to the *tidal radius* configuration, the other, on the right, to the *flex* point of coordinate x_f (see, Tab.1).

Then the flex point will occur at:

$$x_f \simeq \left(4 \frac{2-d}{1-d}\right)^{\frac{1}{3-d}} x_t \quad (43)$$

It should be noted that the flex point may exist only if $d < 1$ and that it occurs at x_t times a factor $f = \left(4 \frac{2-d}{1-d}\right)^{\frac{1}{3-d}}$ (see, Tab.1) which depends only on the exponent d and which changes in a monotonic way from 2 to ∞ as d increases from 0 to 1.

We now turn back on the question, opened at the end of the previous section, related to the dependence of the non-monotonic character of the luminous Clausius' virial energy, and of the location of its maximum, on the approximations used. As we have seen the approximated expressions of energies tend to the rigorous ones as soon as the $\xi_c \rightarrow 0$. Then we have to explore what happens when the core dimensions in the two components decrease. In accordance with our previous discussion on this point (see, sect.A.2 in LS), we again conclude that, if the exponent b is not too high ($b < 2$) and the two power-law exponents satisfy the constraints given by (A.8), the maximum on the V_B trend appears and its coordinate x_t changes very little as $\xi_c \rightarrow 0$. As

Table 1

The most important physical parameters in the energy trends of figures. The common curve parameters are: $\xi_c = 0.01$, $m = 8.5$; $x_t = a_t/a_D$; x_f marks the ratio a_B/a_D at which the variation of total potential energy of the B -component reaches its minimum (the flex, eq.43); x'_f marks the flex coordinate for the total potential energy of the whole system (eq.55). $f = x_f/x_t$.

| cases | b | d | x_t | f | x_f | $3x_t$ | x'_f |
|-------|-----|-----|-------|-------|-------|--------|--------|
| 1) | 0.0 | 0.0 | 0.389 | 2.000 | 0.778 | 1.167 | 0.590 |
| 2) | 0.0 | 0.5 | 0.346 | 2.702 | 0.935 | 1.039 | 0.708 |
| 3) | 0.5 | 0.5 | 0.361 | 2.702 | 0.975 | 1.083 | 0.739 |
| 4) | 1.5 | 0.5 | 0.425 | 2.703 | 1.149 | 1.274 | 0.871 |

soon as $2 \lesssim b < 2.5$ the maximum also exists under the limitations (A.8), but its location moves towards $x = 1$ with $\xi_c \rightarrow 0$, by reaching a limit coordinate which is always less than 1. When $2.5 \leq b < 3$ and again the limitations (A.8) are satisfied, the maximum appears if ξ_c is not too small. Its coordinate x_t moves towards 1 as soon as ξ_c decreases and then it disappears as $\xi_c \rightarrow 0$ (in the case of, $b=2.5$, which happens at $\xi_c = 0.00038$). These last two results are something new to add to the previous analysis. Then the following warning has to be pointed out: the non-monotonic character of V_B , may be lost¹ if the dimensions of the homogeneous cores become very small with $2.5 \leq b$, even if the conditions (A.8) are fulfilled. To have or not to have the divergency at the center of the two configurations, seems to become an essential feature in order to obtain or not an induced scale length on the inner component. This new message again requires, with the observations made at the beginning of the previous section, a further paper on this matter.

¹ It may be conserved from a mathematical point of view, but the maximum corresponds to a non-physical configuration in our model, because it occurs at $x_t > 1$.

6 Thermodynamical arguments

To underline as special is the *tidal radius configuration* we will consider here some aspects of the thermodynamics related to the luminous component. As well known (Chandrasekhar 1939) when a single virialized component evolves through a quasi-static sequence of contractions, it has to lose an heat amount, ΔQ , which is one half of the variation of its self potential energy due to the contraction, in the meanwhile the other half goes to heat the structure. That means we need of a dissipation mechanism (e.g., gas cloud collisions) and of cooling processes. The consequence will be a local decreasing of the structure entropy and a corresponding increase of the universe entropy according to the I° thermodynamic principle (Secco 1999). Now, the question is: what happens if we take into account the contraction process of the same component (B) if it is embedded inside an other non-dissipative one (D)? In order to answer the question we have to re-consider the two fundamental equations: 1) the first thermodynamic Principle applied to B system and ii) the variation of the virial quantities of the same component during a quasi-static transition. In the I° Principle equation it has to appear now the work done by both the forces on the system: the self gravity and the gravity which the dark matter distribution exerts on it. The corresponding potential energy variation for a small contraction will be ΔV_B . Combining the two equations and considering that the internal energy is the total kinetic energy of the system, T_B , (Schwarzschild 1958), we obtain:

$$\Delta Q = \Delta V_B/2 \quad (44)$$

$$\Delta T_B = -\Delta V_B/2 \quad (45)$$

where ΔQ is the amount of heat exchanged between the system and the universe. Again the two requests that the system settles again in virial equilibrium and obeys to the I° Principle yields the equipartition of the Clausius' virial energy variation that is one half of it has to be exchanged with the Universe, the other half has to contribute to change the "temperature" of the system which is proportional to the total kinetic energy. The result is formally the same found for the single component for which the Clausius' virial energy coincides with the self potential energy, but the difference for the B component inside the D one is that the potential energy V_B now is a non-monotonic function of x (Fig.1). The consequence is that the differential eq.(44) becomes the following:

$$\Delta \tilde{Q} = \frac{1}{2} \left(\frac{\nu_{\Omega B}}{x^2} - \nu'_V m(2-d)x^{1-d} \right) \Delta x \quad (46)$$

where $\Delta\tilde{Q}$ is the exchanged amount of heat in normalized units (see, eq.23) and Δx the normalized variation of the B structure semimajor axis. Moreover, by defining the entropy variation of the B system, in arbitrary units, as:

$$\Delta\tilde{S} = \frac{1}{\tilde{T}_B} \Delta\tilde{Q} \quad (47)$$

The eqs.(47) and (23) yield:

$$\Delta\tilde{S} = \left(\frac{\frac{\nu_{\Omega B}}{x^2} - \nu'_V m(2-d)x^{1-d}}{\frac{\nu_{\Omega B}}{x} + \nu'_V m x^{2-d}} \right) \Delta x \quad (48)$$

where $\tilde{T}_B = -\frac{1}{2}\tilde{V}_B$, according to eq.(1). It is easy to see that the derivative of heat is stationary at $x = x_t$, and as consequence also the derivative of the B entropy. Then we have to wait a minimum or a maximum of the entropy of the luminous component at the *tidal radius configuration*. Indeed, the integration of eq.(48) yields always a non-monotonic trend for the function $\tilde{S}(x)$ with a maximum at the *tidal radius*, as soon as the the maximum in Clausius' virial energy does exist. In the special case of Tab.1, $b = 0$; $d = 0.5$, we obtain:

$$\tilde{S}(x) - \tilde{S}(1) = \ln(12539) - \ln\left(\frac{11339 x^{5/2} + 1200}{x}\right) \quad (49)$$

Its trend is shown in Fig.3.

The existence of this entropy maximum is able to stress the relevance of the Clausius' energy maximum. Indeed, according to Layzer (1976), the definition of thermodynamic information is :

$$I = S_{max} - S \quad (50)$$

where S_{max} means the maximum value the entropy of the system may have as soon as the constraints on it, which fix the actual value of its entropy to S , are relaxed. Then, in order to increase its information a system has to decrease its entropy in respect to that of the universe. For a luminous component as B , which is embedded in an other D , a contraction decreases the entropy of B only if its dimension is smaller or equal to a_t . It means that only from this dimension downwards the component B may gain information during its evolution due to dissipation until to become more structured by changing its gas amount into stars (Secco 1999). Even if the argument has to make wider and deeper in a future work it seems to us it may become the ground for the interpretation of the oserved cut-off radius observed in many edge-on spiral galaxies (see, e.g., van der Kruit, 1979; Pohlen et al. 2000a, 2000b and Kregel et al., 2002). From a preliminary analysis the observed cut-off adius correlates

with the B mass as the tidal radius does (Guarise et al. 2001; Secco & Guarise 2001).

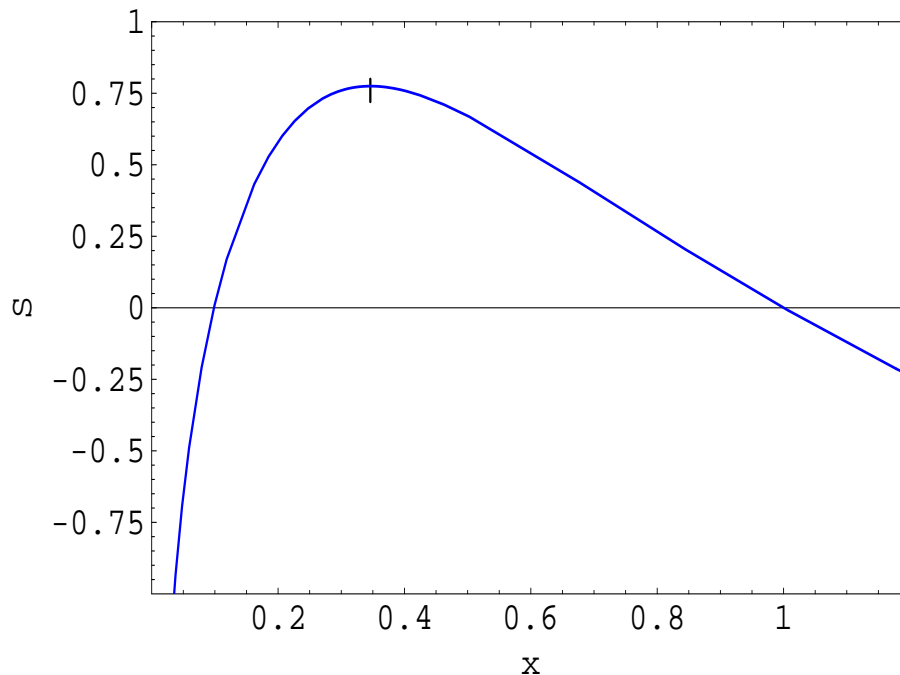


Fig. 3. Entropy trend of the B -system, in arbitrary units, as function of x (case 2 of Tab.1). The normalized factor is the same of the other figures. The maximum occurs at the *tidal radius* $x_t = 0.346$.

7 DM energy trends

By looking at Fig.4 which shows the energy trends of the D -component, the non-specularity of the virial energies behavior between the two components is manifest. Indeed, \tilde{V}_D is monotonic (curve a), moreover $(\tilde{E}_{pot})_D$ increases very slowly at decreasing x .

It should be underlined that the two energies become equal as soon as the residual energies, given by the eq.(30), are zero. That occurs at the configuration characterized by the size ratio:

$$x_o \simeq \left[\frac{(3-d)}{(3-b)} \frac{[5-(b+d)]}{(5-2d)} \right]^{\frac{1}{2-d}} \quad (51)$$

If the mass distributions of the two components are the same ($b = d$), the equality appears only when the two configurations are coinciding ($x_o = 1$). In the cases of different mass distributions, it may be possible to find that the virial energy becomes equal to the potential energy only at one configuration

which satisfies the physical condition: $0 < x < 1$; in turn, that means :

$$(2 - d)(b - d) < 0$$

i.e., $b < d$ (the case of the Fig.4), if we have taken into account the dynamics of two-component system at the presence of a tidal radius ($d < 2$). Then, the difference between the energies, at $x = 1$, becomes:

$$(\tilde{Q}_{BD})_{x=1} = -(\tilde{Q}_{DB})_{x=1} \simeq \frac{1}{2} \nu'_V m \frac{(b - d)}{(3 - b)} \quad (52)$$

All that is true not only for the D -component but, of course, also for the B -one, due to the anti-symmetric nature of the residual terms.

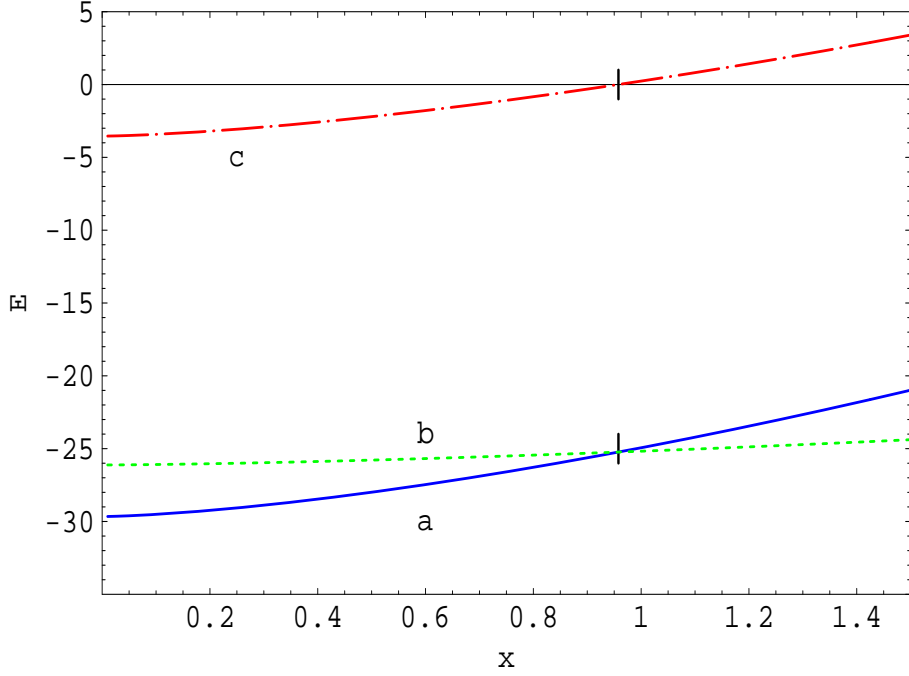


Fig. 4. The trends of the D -system energies, as function of x (case 2) of Tab.1), normalized as in the previous figures. The a-curve (solid line) and the b-one (dotted line) represent the behavior of the Clausius' virial, \tilde{V}_D , and of the total potential energy $(\tilde{E}_{pot})_D$, respectively ; the c-curve (dash dotted -line) shows the trend of the residual energy $\tilde{Q}_{DB} = -\tilde{Q}_{BD}$. The two energies are equal at $x_o = 0.9579$ (the vertical mark) and the score at $x = 1$, is: $(\tilde{Q}_{DB})_{x=1} = 0.2361$, eq.(52).

8 The energies of the whole system

In the last step we will investigate the potential energy trend of the whole system, which means the trend of the function (34) at decreasing x . It is shown

in Fig.5. Again a flex point appears. Indeed, the first and second derivative turn out to be, respectively:

$$\frac{d\tilde{E}_{pt}}{dx} \simeq \frac{\nu_{\Omega_B}}{x^2} + \nu'_V m x^{1-d} \quad (53)$$

$$\frac{d^2\tilde{E}_{pt}}{dx^2} \simeq -2\frac{\nu_{\Omega_B}}{x^3} + \nu'_V m \frac{1}{x^d}(1-d) \quad (54)$$

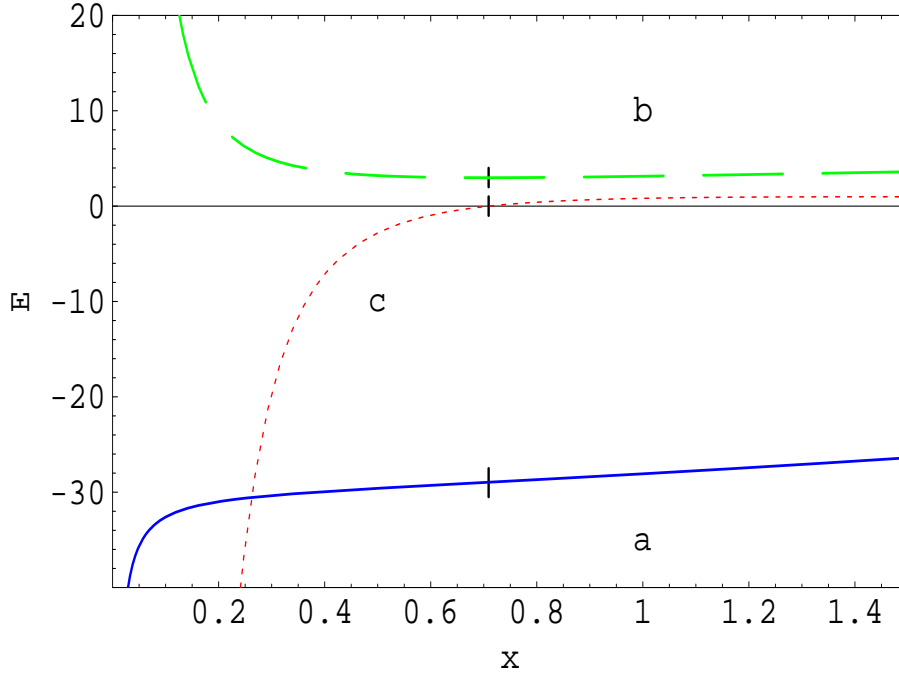


Fig. 5. The potential energy trend of the whole $(B + D)$ -system, normalized to the usual factor. The a-curve (solid line) represents the total potential energy, \tilde{E}_{pt} ; the b (dashed line) and c-curve (dotted line) represent the first and second derivative of the total potential energy, respectively. The curve parameters are those of the case 2) in Tab.1. The flex point of eq.(55) is marked.

Then the flex point will occur for:

$$x'_f \simeq \left(2\frac{2-d}{1-d}\right)^{\frac{1}{3-d}} x_t = x_f / 2^{1/(3-d)} \quad (55)$$

It should be noted that again the flex point may exist only if $d < 1$ and it is located a factor $1/2^{\frac{1}{3-d}}$ before the flex point of $(\tilde{E}_{pot})_B$.

The total potential energy trend of Fig.5 for the whole system is also that of its total mechanical energy when it is in virial equilibrium. Indeed, according

to eq.(9), we have:

$$E_{mec} = E_{pt} + T_B + T_D = V_B + V_D - \frac{1}{2}V_B - -\frac{1}{2}V_D = \frac{1}{2}E_{pt} \quad (56)$$

The result is different for the single u-subsystem. From eqs.(5,6) we obtain:

$$(E_{mec})_u = (E_{pot})_u + T_u = \Omega_u + W_u - \frac{1}{2}V_u = \frac{1}{2}V_u - Q_{uv} \quad (57)$$

The trends of the u-mechanical energies are given in Fig.6. It is difficult to look for a physical meaning related to the small increase of the mechanical energy of the D component as x decreases (c curve). It is probably due to the artificial constraint, we have considered, that the dark matter system has a size and a mass distribution insensitive to the contraction of the baryonic component which occurs inside. As already pointed out by Barnes & White (1984), there is an iduced effect from B density distribution on the inner regions of dark halo which, even if non-dramatic, might change the coefficient $\nu_{\Omega D}$, $(\nu_D)_M$ and then ν'_V .

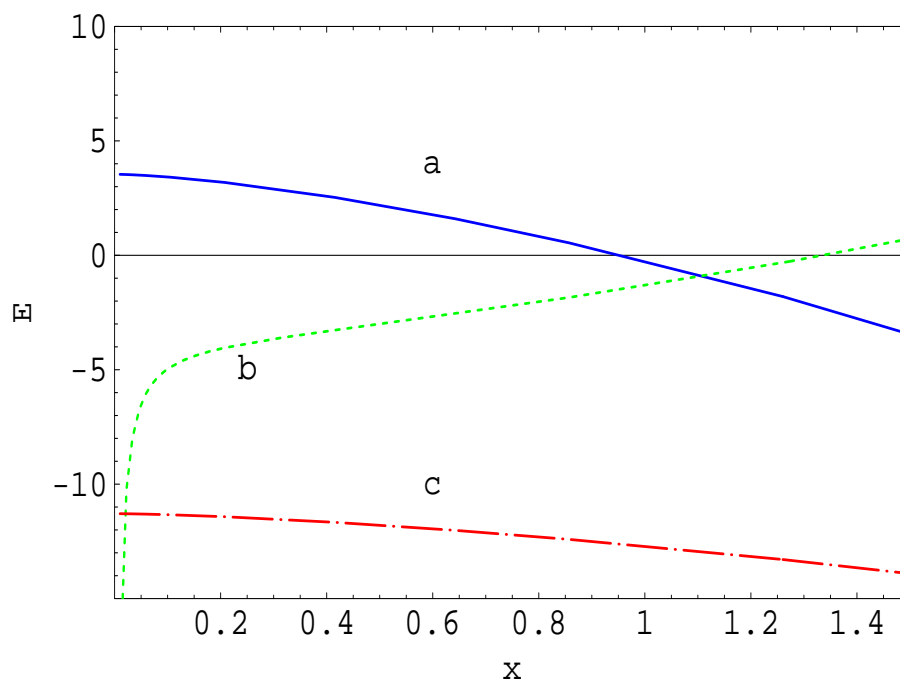


Fig. 6. The mechanical energy trends of the u-subsystem, given by the eq.(57), normalized to the usual factor. The b (dotted line), c-curve (dash dotted-line) and a-curve (solid) represent the $(\tilde{E}_{mec})_B$, $(\tilde{E}_{mec})_D$ and the residual energy \tilde{W}_{BD} , respectively. The curve parameters are those of the case 2) in Tab.1.

9 Discussion and Conclusion

The energetics of a two-component virial system has been analyzed during its dynamic evolution due to the contraction of a inner (baryonic) component inside an outer of dark matter, which is assumed, for sake of simplicity, to be fixed. The results are also compared with those we obtain without the presence of the dark potential well. The analysis was done with the help of some simple, good approximate expressions for all the energies (in the cases of $b < 2$ and with $\xi_c = 0.01$) which, once the form factor is assigned, are only functions of the b and d exponents in the two power-law density distributions. The different character between the energy trends of Clausius' virial and of the total potential energy for the baryonic (or bright component B), has been underlined and the physical main consequences has been derived for the minimum of the virial energy. The particular location of the special B size corresponding to the minimum (*tidal radius*) on the total potential energy curve and the discover of one flex point on it, has stressed the character of the *tidal radius* as a scale length induced by the dark matter halo component on the gravitational field of the inner baryonic one. This scale length marks the beginning of the two different regimes as follows: the self-energy regime, when $x < x_t$, and the tidal-energy regime at about $3x_t$.

We claim as observable counter-parties of these theoretical reasons for the real existence of this induced scale length, at least the two followings: the first one is more direct: it is the cut-off radius observed in many edge-on spiral galaxies. Thermodynamical arguments related to the presence of an entropy maximum at this scale length and some preliminary comparison between correlations from observables and theoretical expectations seem to prove the connection. The other one is more indirect but it has an important, observable consequence: if there is this length, we are able to reproduce some of the main features of the Fundamental Plane (FP) for the elliptical galaxies (LS1). From a general point of view, the two arguments are connected by the thermodynamics in the following way: the elliptical galaxies stay on the maximum entropy stage without a significant structure evolution, the cut-off spirals, practically, begins their evolution from this stage forwards.

How the main physical results depend on the approximations used has also been considered. The main result is that: a too small homogeneous cores in both the two subsystems might cancel this induced length as soon as $b \geq 2.5$. Avoiding the divergency at the center of the two configurations, seems to become an essential condition in order to obtain the FP features. Here we are constrained by the restriction of handling together the two cores and then we need of a further paper on this matter in order to disentangle the probable different core-dimension play.

Nevertheless, from this point of view an appealing application to the galaxy clusters may be thought of. If we take into account the values of the exponent α , used by Girardi et al.(1995) in the power-laws which give the best fit for the galaxy distributions, at a distance $r \gg R_c$ (R_c = core radius), in the clusters, we can see that the corresponding range of our exponent b turns out to be approximately the critical one we have found in the section (5), $2.5 \leq b < 3$, with ratios R_c/R_{vir} (our ξ_c) which are big enough for obtaining the maximum virial energy at $x < 1$.

The energies of the D -subsystem were also considered. Its total potential energy is practically unaffected by the contraction of the B -subsystem whereas the virial energy slowly increases, in absolute value, as x decreases. The conditions to obtain the equality between these two energies was with the main result that only one configuration may enjoy this property. It corresponds to the initial one, when the two substructures fill the same volume, only if the two mass distributions are the same.

Finally the trend of the potential energy of the whole system tells us that a configuration exists of minimum variation of the total potential energy (and then of the total mechanical energy), a flex point, inside its monotonic behavior. The conditions required in order to obtain either the flex on the B total potential energy, or on the total potential energy of the whole system were investigated and the result again is a constrain only on the dark matter distribution (see the *tilt* of the FP). The mechanical energies either of the whole system or of both the subsystems were also taken into account.

Even if we are aware that the next step we have to do is to investigate the energetics of a two-component system with or without central divergencies and characterized by two more realistic density distributions, e.g., of Hernquist (1990) kind for the inner component and of Zhao (1996) general kind for the dark matter halo (included the NFW profile (Navarro et al., 1997)), as already considered, e.g., by Caimmi & Marmo (2002), the present results seem to be very attractive for the future work.

Acknowledgements

We thank our friend, Prof. R. Caimmi for helpful discussions and mathematical support.

A Appendix

According to RC we define:

$$w^{int}(x) = L(\xi_c, x) + M(\xi_c, x) \quad (\text{A.1})$$

$$w^{ext}(x) = G(\xi_c, x) + H(\xi_c, x) \quad (\text{A.2})$$

$$L(\xi_c, x) = \int_0^{\xi_c} F_D \frac{dF_B}{d\xi_D} \xi_D d\xi_D \quad (\text{A.3})$$

$$M(\xi_c, x) = \int_{\xi_c}^x F_D \frac{dF_B}{d\xi_D} \xi_D d\xi_D \quad (\text{A.4})$$

$$G(\xi_c, x) = \int_0^{\xi_c} F_B \frac{dF_D}{d\xi_D} \xi_D d\xi_D \quad (\text{A.5})$$

$$H(\xi_c, x) = \int_{\xi_c}^x F_B \frac{dF_D}{d\xi_D} \xi_D d\xi_D \quad (\text{A.6})$$

The two functions $F_B(\xi_B = \frac{a_D}{a_B} \xi_D)$ and $F_D(\xi_D)$ in the ranges $(0, \xi_c)$ and (ξ_c, x) , for different values of exponents b and d , are given in Tab.3 of Appendix A in LS, with the assumption that $(\xi_c < \frac{a_B}{a_D})$.

In Table 1 of Appendix A (LS1), the corresponding functions $L(\xi_c, x)$ and $M(\xi_c, x)$ are shown with the approximate analytical expressions of $w^{int}(x)$ we will use in the next sect.. In Table 4 of Appendix A (LS), the corresponding functions $G(\xi_c, x)$ and $H(\xi_c, x)$ are given with the approximate analytical expressions of $w^{ext}(x)$ which we will also need. We take into account the approximation of w^{ext} , towards which all the exact analytic expressions of it converge, by disregarding terms of higher order in respect to ξ_c at a different degree (see Table 4 in Appendix A of LS), which is:

$$w^{ext}(\frac{a_B}{a_D}) \simeq w_{prox}^{ext} = -\frac{4\xi_c^{b+d}}{(3-d)[5-(b+d)]}(\frac{a_B}{a_D})^{3-d} \quad (\text{A.7})$$

despite the b and d values, provided the following limitations hold:

$$0 \leq b < 3 ; 0 \leq d < 2 \Rightarrow (b+d) < 5 \quad (\text{A.8})$$

These limitations also ensure that the tidal and the self potential-energy tensor have the same sign, in all the cases we take into account. In order to highlight the D mass fraction, $\widetilde{M}_D = M_D(\frac{a_B}{a_D})^{3-d}$, which exerts dynamic effects

on B according to Newton's theorem (the equivalent of M_D^* defined for the homogeneous case, see LS), we define the factor:

$$\nu'_V = \frac{9}{2}[(\nu_B)_M(\nu_D)_M]^{-1} \frac{\xi_c^{b+d}}{(3-d)[5-(b+d)]} \quad (\text{A.9})$$

In this way it follows that:

$$\nu_V \simeq \nu'_V \frac{M_D}{M_B} \left(\frac{a_B}{a_D}\right)^{3-d} \quad (\text{A.10})$$

Moreover under the limitations given by the (A.8), the following approximation also holds (see LS1):

$$w^{int}\left(\frac{a_B}{a_D}\right) \simeq \frac{4\xi_c^{b+d}}{(2-d)[5-(b+d)]} \left(\frac{a_B}{a_D}\right)^{3-d} - \frac{4\xi_c^{b+d}}{(2-d)(3-b)} \left(\frac{a_B}{a_D}\right) + \epsilon \quad (\text{A.11})$$

$$\epsilon = -4 \frac{\xi_c^{d+3}}{(2-d)3} \left(\frac{a_D}{a_B}\right)^2 \delta \quad (\text{A.12})$$

$$\delta = \left[1 - \frac{3}{3-b} \left(\frac{a_B}{a_D}\right)^b\right] \quad (\text{A.13})$$

As we have already underlined (LS1) in case $b = 0$, δ and then ϵ of eq.(A.11) become 0, whatever the value of d may be, and that the relevance of ϵ , in respect to the other terms of the same equation, increases quickly, at fixed d , as soon as b increases. Moreover, at fixed b , the weight of ϵ grows as d increases, even if less than before; at fixed b and d the contribution of ϵ increases as the ratio a_B/a_D becomes smaller. If we limit ourselves to choosing $b \leq 1.5$ and $d \simeq 0.5$, we may disregard ϵ in the approximation of w^{int} with a maximum error of 12% when $b = 1.5$ and a_B/a_D decreases to 0.4. That occurs if we choose $\xi_c = 0.1$, but the error decreases as ξ_c decreases.

It should be noted that the approximation of w^{int} is different from that of w^{ext} , even if the core dimensions ξ_c , are the same, because of the b value. Indeed, for $2 \lesssim b$ one needs to introduce in the approximated w^{int} the term δ in which the ratio a_B/a_D has b as exponent. That does not appear in the w^{ext} approximation.

By also taking into account the approximation of eq.(A.7) the following relation holds, as soon as ϵ is negligible:

$$w^{int} \simeq -\frac{4\xi_c^{b+d}}{(2-d)(3-b)} \left(\frac{a_B}{a_D}\right) - w^{prox} \frac{(3-d)}{(2-d)} \quad (\text{A.14})$$

By using eq.(A.14), ($\epsilon \simeq 0$), we obtain the following approximation for the coefficient of eq.(18), as a function of ν'_V :

$$\nu_{VD} \simeq \nu'_V \frac{1}{m} \frac{3-d}{2-d} \left\{ \frac{5-(b+d)}{3-b} - \left(\frac{a_B}{a_D} \right)^{2-d} \right\} \quad (\text{A.15})$$

References

- Barnes, J., & White, S.D.M. 1984, *Mont.Not.*, 211, 753
Caimmi R., 1993, *ApJ* 419, 615.
Caimmi R., 1994, *Ap.S.S.* 219, 49.
Caimmi R. & Marmo C., 2002, *NewA* accepted.
Caimmi R. & Secco L., 1992, *ApJ* 395, 119.
Caimmi R. & Secco L., 2001, *ASP Conf. Ser.*, *Galaxy Disks and Disk Galaxies*, Vol.230, Funes, J.G., Corsini, E.M.(Eds), ASP, San Francisco, p.573.
Chandrasekhar S., 1939, *Stellar Structure*, Dover Publications, Inc.
Girardi, M., Biviano, A., Giuricin, G., Mardirossian, F., & Mezzetti, M., 1995, *ApJ*, 438, 527.
Guarise G., Galletta G., & Secco L., *Astr. Gesellschaft, Jenam 2001, Abstract Series*, 18, 202.
Hernquist, L., 1990, *Apj*, 356,359.
Hoerner, V.S., 1958, *ZA* 44, 221.
Kregel, M., van der Kruit, P.C., & Grijs, R., 2002, *MNRAS*, (astro-ph/0204154).
Layzer D., 1976, *ApJ*, 206, 559
Navarro, J.F., Frenk, C.S., White, S.D.M. 1997, *Apj*,490,493.
Pohlen M., Dettmar R.-J., Lütticke R., & Schwarzkopf U., 2000a, *A&AS* 144, 405.
Pohlen M., Dettmar R.-J. & Lütticke R., 2000b, *A&A* 357, L1-L4.
Schwarzschild M. 1958, *Structure and Evolution of the Stars*, Dover
Secco L., 1999, *ASP Conf. Ser.*, *Observational Cosmology: The Development of Galaxy Systems*, Vol.176, Giuricin, G., Mezzetti, M., Salucci, P. (Eds.), ASP, San Francisco, p.449.
Secco L., 2000, *NewA* 5, 403.
Secco L., 2001, *NewA* 6, 339.
Secco L. & Guarise G., *Astr. Gesellschaft, Jenam 2001, Abstract Series*, 18, 208.
van der Kruit P.C., 1979, *A&AS* 38,15.
Zhao, H.S. 1996, *MNRAS*, 278, 488.